

Light cone wave functions in the context of space like transition form factors and prompt hadroproduction of η_c ($1S, 2S$)

Izabela Babiarz

The Henryk Niewodniczański Institute of Nuclear Physics
Polish Academy of Sciences, Kraków

Środowiskowe Seminarium Fizyki Wysokich Energii "Biały Błasówka"
Kraków, 27 Maj 2022



THE HENRYK NIEWODNICZAŃSKI
INSTITUTE OF NUCLEAR PHYSICS
POLISH ACADEMY OF SCIENCES

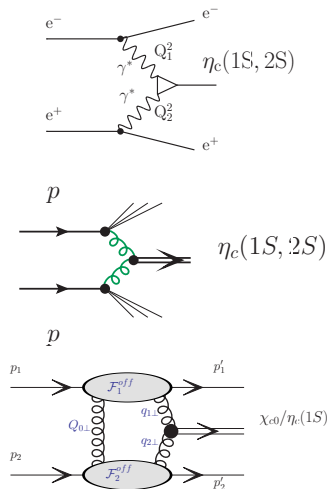
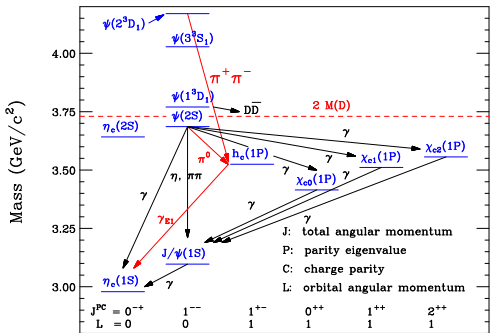


POLISH NATIONAL AGENCY
FOR ACADEMIC EXCHANGE

Contents

- Introduction
- Description of the $\gamma^*\gamma^* \rightarrow \eta_c(1S,2S)$ transition
- Nonrelativistic quarkonium wave functions
- Light-front quarkonium wave functions
- $F(0,0)$ transition for both on-shell photons
- Transition form factor $F(Q_1^2, Q_2^2)$ for $\gamma^*\gamma^* \rightarrow \eta_c(1S,2S)$
- Relation between distribution amplitudes and quarkonium wave functions
- The evolution of the distribution amplitudes
- Prompt η_c production in the k_\perp -factorisation approach
- Central exclusive production of charmonia
- Conclusions

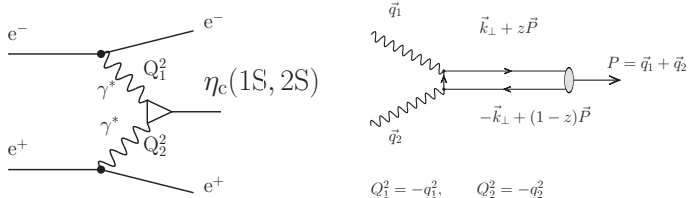
Introduction



- Charmonia with even charge parity ($c\bar{c}$ states) : prompt production via gluon-gluon fusion.
- Quarkonia can provide a good test for unintegrated gluon densities.

Description of the mechanism $\gamma^*\gamma^* \rightarrow \eta_c(1S, 2S)$

Production of η_c in the double-tagged mode of e^+e^- collisions measures the $\gamma^*\gamma^* \rightarrow \eta_c(1S, 2S)$ transition form factor.



$$\mathcal{M}_{\mu\nu}(\gamma^*(q_1)\gamma^*(q_2) \rightarrow \eta_c) = 4\pi\alpha_{\text{em}} (-i)\varepsilon_{\mu\nu\alpha\beta} q_1^\alpha q_2^\beta F(Q_1^2, Q_2^2)$$

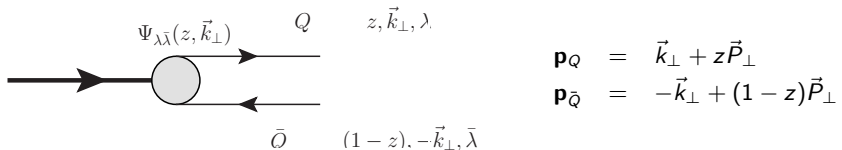
The light-cone representation of the transition form factor:

$$F(Q_1^2, Q_2^2) = e_c^2 \sqrt{N_c} 4m_c \cdot \int \frac{dz d^2\kappa}{z(1-z)16\pi^3} \psi(z, \kappa) \times \left\{ \frac{1-z}{(\kappa - (1-z)\mathbf{q}_2)^2 + z(1-z)\mathbf{q}_1^2 + m_c^2} + \frac{z}{(\kappa + z\mathbf{q}_2)^2 + z(1-z)\mathbf{q}_1^2 + m_c^2} \right\}.$$
$$Q_i^2 = \mathbf{q}_i, \vec{k}_\perp \equiv \kappa$$

The construction of the $\gamma^*\gamma^*\rightarrow\eta_c$ form factor

The general form of the amplitude \Rightarrow the invariant form factor:

$$\frac{1}{4\pi\alpha_{\text{em}}}\mathcal{M}_{\mu\nu}(\gamma^*(q_1)\gamma^*(q_2)\rightarrow\eta_c) = (-i)\varepsilon_{\mu\nu\alpha\beta}q_1^\alpha q_2^\beta F(Q_1^2, Q_2^2)$$



Frame-independent $Q\bar{Q}$ component from LF-Fock-state expansion:

$$|\text{Meson}; P_+, \vec{P}_\perp\rangle = \sum_{i,j,\lambda,\bar{\lambda}} \frac{\delta_j^i}{\sqrt{N_c}} \int \frac{dz d^2\vec{k}_\perp}{z(1-z)16\pi^3} \Psi_{\lambda\bar{\lambda}}(z, \vec{k}_\perp) |Q_i\lambda(zP_+, \mathbf{p}_Q)\bar{Q}_j^i((1-z)P_+, \mathbf{p}_{\bar{Q}})\rangle + \dots$$

$Q\bar{Q}$ interaction potential model

$$\frac{\partial^2 u(r)}{\partial r^2} = (V_{\text{eff}}(r) - \epsilon)u(r), \quad u(r) = rR(r), \quad \epsilon = m_Q E, \quad V_{\text{eff}} = m_Q V(r) + \frac{\ell(\ell+1)}{r^2}$$

$Q\bar{Q}$ interaction potential models:

- ① **Buchmüller-Tye**, $m_c = 1.48 \text{ GeV}$, $m_b = 4.87 \text{ GeV}$,

$$V(r) = \begin{cases} \frac{k}{r} - \frac{8\pi}{27} \frac{v(\lambda r)}{r}, & r \geq 0.01 \text{ fm} \\ \frac{-16\pi}{25} \frac{1}{r \ln(w(r))} \left(1 + 2\left(\gamma_E + \frac{53}{75}\right) \frac{1}{\ln w(r)} - \frac{462}{625} \frac{\ln \ln(w(r))}{\ln(w(r))}\right), & \leq 0.01 \text{ fm} \end{cases}$$

- ② **Cornell**, $m_c = 1.84 \text{ GeV}$, $m_b = 5.17 \text{ GeV}$, $V(r) = \frac{-k}{r} + \frac{r}{a^2}$

- ③ **logarithmic**, $m_c = 1.5 \text{ GeV}$, $m_b = 5.0 \text{ GeV}$,

$$V(r) = 0.6635 \text{ GeV} + (0.733 \text{ GeV}) \log(r \cdot 1 \text{ GeV})$$

- ④ **harmonic oscillator** $m_c = 1.4 \text{ GeV}$, $m_b = 4.2 \text{ GeV}$, $V(r) = \frac{1}{4}m_Q \omega^2 r^2$

- ⑤ **power-like**, $m_c = 1.334 \text{ GeV}$ $V(r) = 6.41 \text{ GeV} + (6.08 \text{ GeV})(r \cdot 1 \text{ GeV})^{0.106}$

Nonrelativistic quarkonium wave functions

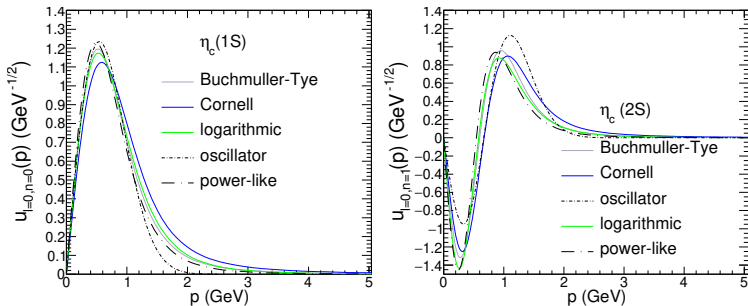


Figure: Radial momentum space wave function for different potentials.

Radial space wave function are obtained from the Schrödinger equation

$$\frac{\partial^2 u(r)}{\partial r^2} = (V_{\text{eff}}(r) - \epsilon)u(r), \quad u(r) = rR(r) \quad , \epsilon = m_Q E, \quad V_{\text{eff}} = m_Q V(r) + \frac{l(l+1)}{r^2}$$

$$\int_0^\infty |u(r)|^2 dr = 1 \quad \Rightarrow \quad u(p) = \sqrt{\frac{2}{\pi}} \int_0^\infty \sin(pr) u_{00}(r) dr$$

Light-cone wave functions from rest-frame

- Terentev prescription

Rest-frame wave functions for $J = 0$:

$$\Psi_{\tau\bar{\tau}}(\vec{k}) = \underbrace{\frac{1}{\sqrt{2}} \xi_Q^{\tau\dagger} \hat{\mathcal{O}} i\sigma_2 \xi_{\bar{Q}}^{\bar{\tau}*}}_{\text{spin-orbit}} \underbrace{\frac{u_L(k)}{k}}_{\text{radial}} \frac{1}{\sqrt{4\pi}};$$

$$\text{where } \hat{\mathcal{O}} = \begin{cases} \mathbb{I} & \text{spin-singlet, } S = 0, L = 0. \\ \frac{\vec{\sigma} \cdot \vec{k}}{k} & \text{spin-triplet, } S = 1, L = 1. \end{cases}$$

mapping RF momentum to LC representation:

$$\vec{p} = (\vec{k}_\perp, k_z) = (\vec{k}_\perp, \frac{1}{2}(2z - 1)M_{c\bar{c}}), M_{c\bar{c}}^2 = \frac{\vec{k}_\perp^2 + m_Q^2}{z(1-z)},$$

$$\psi(z, \vec{k}_\perp) = \frac{\pi}{\sqrt{2M_{c\bar{c}}}} \frac{u(p)}{p}.$$

Light-cone wave functions from rest-frame - Terentev prescription

Melosh-transf. of spin-orbit part:

$$\xi_Q = R(z, \vec{k}_\perp) \chi_Q, \quad \xi_Q^* = R^*(1-z, -\vec{k}_\perp) \chi_Q^*,$$

$$R(z, \vec{k}_\perp) = \frac{m_Q + zM - i\vec{\sigma} \cdot (\vec{n} \times \vec{k}_\perp)}{\sqrt{(m_Q + zM)^2 + \vec{k}_\perp^2}}$$

$$\hat{O}' = R^\dagger(z, \vec{k}_\perp) \mathcal{O} i\sigma_2 R^*(1-z, -\vec{k}_\perp) (i\sigma_2)^{-1}$$

using properties of Pauli-matrices $i\sigma_2 \vec{\sigma}^* (i\sigma_2)^{-1} = -\vec{\sigma}$

$$\hat{O}' = R^\dagger(z, \vec{k}_\perp) \hat{O} R(1-z, -\vec{k}_\perp).$$

Light-front wave functions

Pseudoscalar (S-wave)

$$\begin{aligned}\Psi_{\lambda\bar{\lambda}}(z, \vec{k}_\perp) &= \begin{pmatrix} \Psi_{++}(z, \vec{k}_\perp) & \Psi_{+-}(z, \vec{k}_\perp) \\ \Psi_{-+}(z, \vec{k}_\perp) & \Psi_{--}(z, \vec{k}_\perp) \end{pmatrix} \\ &= \frac{1}{\sqrt{z(1-z)}} \begin{pmatrix} -k_x + ik_y & m_Q \\ -m_Q & -k_x - ik_y \end{pmatrix} \psi(z, \vec{k}_\perp)\end{aligned}$$

Normalisation

$$\begin{aligned}1 &= \int_0^1 \frac{dz}{z(1-z)} \int \frac{d^2 \vec{k}_\perp}{16\pi^3} \sum_{\lambda\bar{\lambda}} |\Psi_{\lambda\bar{\lambda}}(z, \vec{k}_\perp)|^2 \\ &= \int_0^1 \frac{dz}{z(1-z)} \int \frac{d^2 \vec{k}_\perp}{16\pi^3} 2M_{c\bar{c}} \psi(z, \vec{k}_\perp)\end{aligned}$$

Light-cone wave function for Buchmüller -Tye potential model

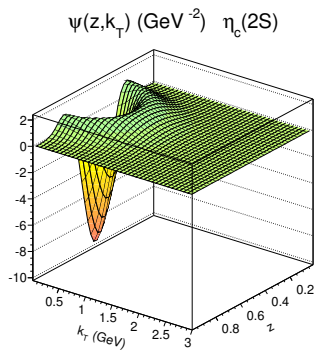
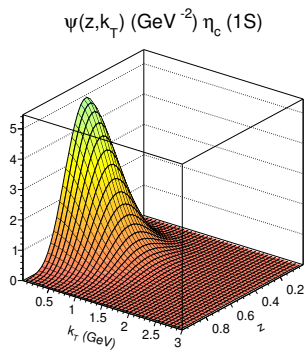


Figure: The light-front wave function $\psi(z, \vec{k}_\perp)$ for Buchmüller-Tye potential.

$F(0,0)$ transition for both on-shell photons

$$F(0,0) = e_c^2 \sqrt{N_c} 4m_c \cdot \int \frac{dz d^2 \vec{k}_\perp}{z(1-z) 16\pi^3} \frac{\psi(z, \vec{k}_\perp)}{\vec{k}_\perp^2 + m_c^2},$$

$F(0,0)$ is related to the two-photon decay width by the formula:

$$\Gamma(\eta_c \rightarrow \gamma\gamma) = \frac{\pi}{4} \alpha_{\text{em}}^2 M_{\eta_c}^3 |F(0,0)|^2.$$

$F(0,0)$ can be rewrite in the terms of radial momentum space wave function $u(k)$:

$$F(0,0) = e_c^2 \sqrt{2N_c} \frac{2m_c}{\pi} \int_0^\infty \frac{dp p u(p)}{\sqrt{M_{c\bar{c}}^3(p^2 + m_c^2)}} \frac{1}{2\beta} \log \left(\frac{1+\beta}{1-\beta} \right),$$

In the non-relativistic (NR) limit, where $p^2/m_c^2 \ll 1$, $\beta \ll 1$, and $2m_c \propto M_{c\bar{c}} \propto M_{\eta_c}$, we obtain

$$F(0,0) = e_c^2 \sqrt{N_c} \sqrt{2} \frac{4}{\pi \sqrt{M_{\eta_c}^5}} \int_0^\infty dp p u(p) = e_c^2 \sqrt{N_c} \frac{4 R(0)}{\sqrt{\pi M_{\eta_c}^5}},$$

where $\beta = \frac{p}{\sqrt{p^2 + m_c^2}}$, the velocity v/c of the quark in the $c\bar{c}$ cms-frame and $R(0)$ radial wave function at the origin.

$F(0,0)$ for both on-shell photons

Transition form factor $|F(0,0)|$ for $\eta_c(1S)$ at $Q_1^2 = Q_2^2 = 0$.

potential type	m_c [GeV]	$ F(0,0) $ [GeV $^{-1}$]	$\Gamma_{\gamma\gamma}$ [keV]	f_{η_c} [GeV]
harmonic oscillator	1.4	0.051	2.89	0.2757
logarithmic	1.5	0.052	2.95	0.3373
power-like	1.334	0.059	3.87	0.3074
Cornell	1.84	0.039	1.69	0.3726
Buchmüller-Tye	1.48	0.052	2.95	0.3276
experiment	-	0.067 ± 0.003 [1]	5.1 ± 0.4 [1]	0.335 ± 0.075 [2]

[1] M. Tanabashi *et al.* [Particle Data Group], Phys. Rev. D **98**, no.3, 030001 (2018).

[2] K. W. Edwards *et al.* [CLEO Collaboration], Phys. Rev. Lett. **86**, 30 (2001) [hep-ex/0007012].

$R(0)$ and $\gamma\gamma$ -width for $\eta_c(1S)$ derived in the non-relativistic limit.

potential type	$R(0)$ [GeV $^{3/2}$]	$\Gamma_{\gamma\gamma}$ [keV] $M = M_{\eta_c}$	$\Gamma_{\gamma\gamma}$ [keV] $M = 2m_c$
harmonic oscillator	0.6044	5.1848	5.8815
logarithmic	0.8919	11.290	11.157
power-like	0.7620	8.2412	10.297
Cornell	1.2065	20.660	13.568
Buchmüller-Tye	0.8899	11.240	11.409

$$f_{\eta_c} \varphi(z, \mu_0^2) = \frac{1}{z(1-z)} \frac{\sqrt{N_c} 4m_c}{16\pi^3} \int d^2k \theta(\mu_0^2 - k^2) \psi(z, k) \text{ and } \int_0^1 dz \varphi(z, \mu_0^2) = 1$$

$F(0,0)$ for both on-shell photons

Transition form factor $|F(0,0)|$ for $\eta_c(2S)$ at $Q_1^2 = Q_2^2 = 0$.

potential type	m_c [GeV]	$ F(0,0) $ [GeV $^{-1}$]	$\Gamma_{\gamma\gamma}$ [keV]	f_{η_c} [GeV]
harmonic oscillator	1.4	0.03492	2.454	0.2530
logarithmic	1.5	0.02403	1.162	0.1970
power-like	1.334	0.02775	1.549	0.1851
Cornell	1.84	0.02159	0.938	0.2490
Buchmüller-Tye	1.48	0.02687	1.453	0.2149
experiment [1]	-	0.03266 ± 0.01209	2.147 ± 1.589	

[1] M. Tanabashi *et al.* [Particle Data Group], Phys. Rev. D **98**, no.3, 030001 (2018).

$R(0)$ and $\gamma\gamma$ -width for $\eta_c(2S)$ derived in the **non-relativistic limit**.

potential type	$R(0)$ [GeV $^{3/2}$]	$\Gamma_{\gamma\gamma}$ [keV] $M = M_{\eta_c}$	$\Gamma_{\gamma\gamma}$ [keV] $M = 2m_c$
harmonic oscillator	0.7402	5.2284	8.8214
logarithmic	0.6372	3.8745	5.6946
power-like	0.5699	3.0993	5.7594
Cornell	0.9633	8.8550	8.6493
Buchmüller-Tye	0.7185	4.9263	7.4374

Normalised transition form factor $F(Q^2, 0)/F(0, 0)$

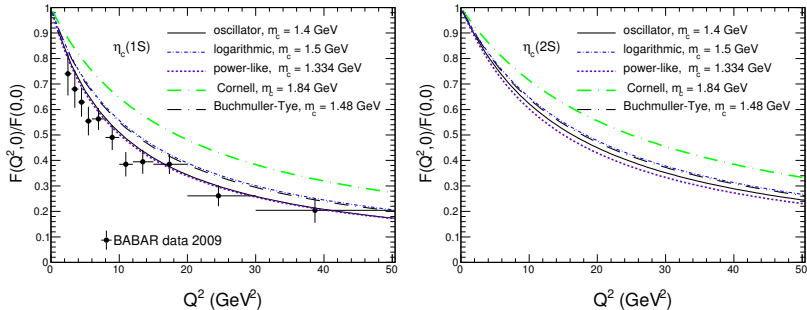


Figure: Normalised transition form factor $F(Q^2, 0)/F(0, 0)$ as a function of photon virtuality Q^2 (I. Babiarz et al. Phys. Rev. D 100 (2019) 5, 054018).
The BaBar data are shown for comparison (J. P. Lees et al. [BaBar Collaboration], Phys. Rev. D 81, 052010 (2010) [arXiv:1002.3000 [hep-ex]]).

Transition form factor $F(Q_1^2, Q_2^2) \gamma^* \gamma^* \rightarrow \eta_c(1S, 2S)$

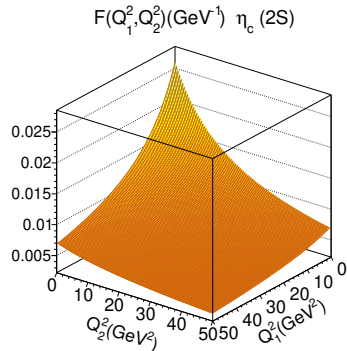
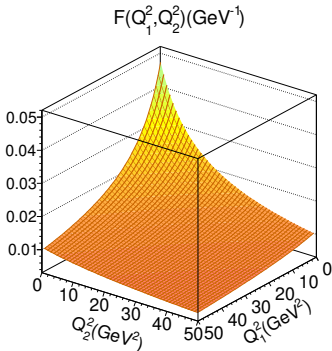


Figure: Transition form factor for $\eta_c(1S)$ and $\eta_c(2S)$ for Buchmüller -Tye potential. The sign of Bose symmetry Q_1^2, Q_2^2 .

Transition form factor $F(\omega, \bar{Q}^2)$

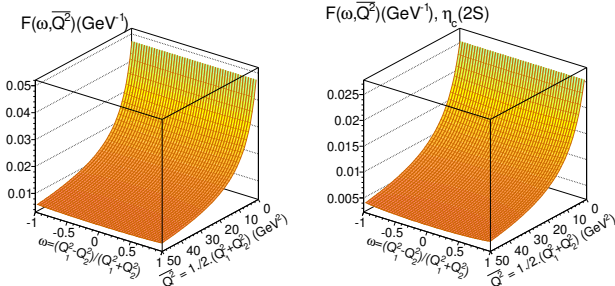


Figure: The $\gamma^* \gamma^* \rightarrow \eta_c$ (1S) and $\gamma^* \gamma^* \rightarrow \eta_c$ (2S) form factor as a function of (Q_1^2, Q_2^2) and (ω, \bar{Q}^2) for the Buchmüller-Tye potential for illustration.

$$\omega = \frac{Q_1^2 - Q_2^2}{Q_1^2 + Q_2^2} \quad \text{and} \quad \bar{Q}^2 = \frac{Q_1^2 + Q_2^2}{2} .$$

Asymptotic behaviour of $Q^2 F(Q^2, 0)$

The rate of approaching of $Q^2 F(Q^2, 0)$ to its asymptotic value predicted by Brodsky and Lepage G. P. Lepage and S. J. Brodsky, Phys. Rev. D 22, 2157 (1980).

$$Q^2 F(Q^2, 0) \rightarrow \frac{8}{3} f_{\eta_c}, \text{ while } Q^2 \rightarrow \infty$$

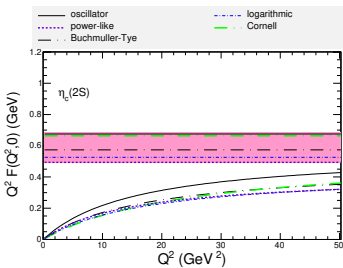
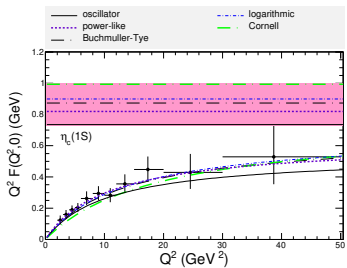


Figure: $Q^2 F(Q^2, 0)$ as a function of photon virtuality Q^2 . Therefore the horizontal lines $\frac{8}{3} f_{\eta_c}$ are shown for reference.

Distribution amplitudes and quarkonium wave functions

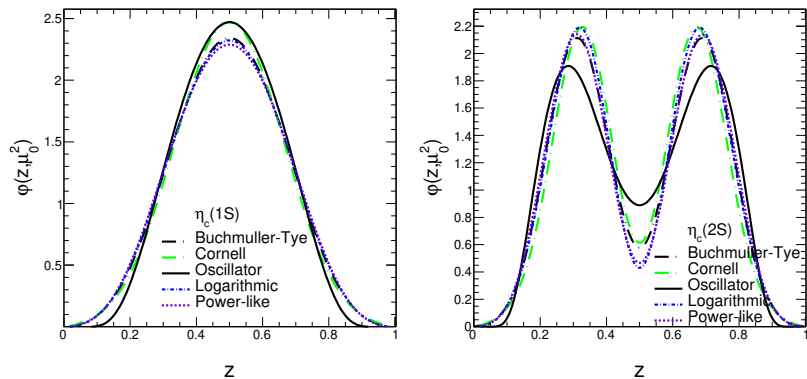


Figure: Distribution amplitudes for different wave functions for η_c (1S) (left panel) and for η_c (2S) (right panel).

$$f_{\eta_c} \varphi(z, \mu_0^2) = \frac{1}{z(1-z)} \int d^2 \vec{k}_\perp \theta(\mu_0^2 - \vec{k}_\perp^2) \psi(z, \vec{k}_\perp)$$

The evolution of the distribution amplitudes

Thanks of the Gegenbauer $C_n^{3/2}$ polynomials we can expand the distribution amplitudes:

$$\varphi(z, \mu^2) = 6z(1-z) \left(1 + a_2(\mu^2) C_2^{3/2}(2z-1) + \dots \right),$$

and then extract the coefficients:

$$a_n(\mu_0) = \frac{2(2n+3)}{3(n+1)(n+2)} \cdot \int_0^1 dz \varphi(z, \mu_0) C_n^{3/2}(2z-1),$$
$$a_n(\mu) = a_n(\mu_0) \cdot \left[\frac{\alpha_s(\mu)}{\alpha_s(\mu_0)} \right]^{\gamma_n/\beta_0}.$$

with the anomalous dimensions γ_n , which can be found for example in *Phys.Rev.D 22 (1980) 2157*

$$\gamma_n = C_F \left(1 - \frac{2}{(n+1)(2+n)} + 4 \sum_{m=2}^{n+1} \frac{1}{m} \right), \quad \beta_0 = \frac{11}{3} N_c - \frac{2}{3} N_f.$$

The evolution of the distribution amplitudes

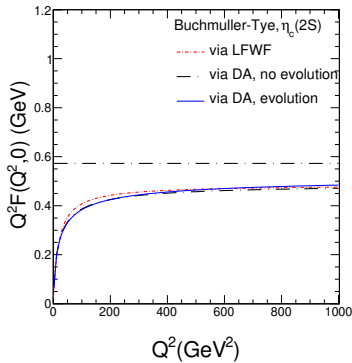
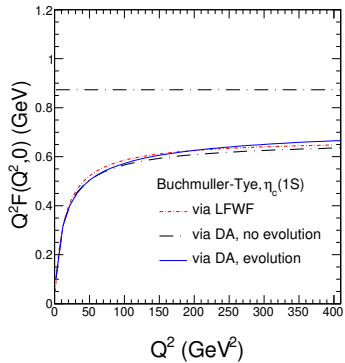
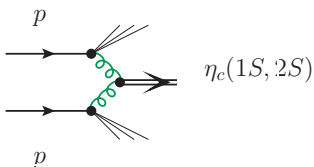


Figure: $Q^2 F(Q^2)$ for η_c (1S)(left panel) and η_c (2S) (right panel) as a function of photon virtuality. The horizontal line is the limit for $Q^2 \rightarrow \infty$, calculated for the Buchmüller-Tye potential.

Hadroproduction of $\eta_c(1S, 2S)$ via gluon-gluon fusion



To the lowest order, it is proportional to the matrix element for the $\gamma^* \gamma^* \rightarrow \eta_c$ vertex. The form factor $I(\vec{q}_{\perp 1}^2, \vec{q}_{\perp 2}^2)$ is related to the $\gamma^* \gamma^* \rightarrow \eta_c$ transition form factor $F(Q_1^2, Q_2^2)$, $Q_i^2 = \vec{q}_{\perp i}^2$ as

$$F(Q_1^2, Q_2^2) = e_c^2 \sqrt{N_c} I(\vec{q}_{\perp 1}^2, \vec{q}_{\perp 2}^2)$$

$$\frac{d\sigma}{dy d^2\vec{p}_\perp} = \int \frac{d^2\vec{q}_{\perp 1}}{\pi \vec{q}_{\perp 1}^2} \mathcal{F}(\mathbf{x}_1, \vec{q}_{\perp 1}^2, \mu_f^2) \int \frac{d^2\vec{q}_{\perp 2}}{\pi \vec{q}_{\perp 2}^2} \mathcal{F}(\mathbf{x}_2, \vec{q}_{\perp 2}^2, \mu_f^2) \\ \times \delta^{(2)}(\vec{q}_{\perp 1} + \vec{q}_{\perp 2} - \vec{p}_\perp) \frac{\pi}{(x_1 x_2 s)^2} |\mathcal{M}|^2$$

where the momentum fractions of gluons are fixed as $x_{1,2} = m_T \exp(\pm y)/\sqrt{s}$.

The off-shell matrix element (we restore the color-indices):

$$\mathcal{M}^{ab} = \frac{q_{1\perp}^\mu q_{2\perp}^\nu}{|\vec{q}_{\perp 1}| |\vec{q}_{\perp 2}|} \mathcal{M}_{\mu\nu}^{ab} = \frac{q_{1+} q_{2-}}{|\vec{q}_{\perp 1}| |\vec{q}_{\perp 2}|} n_\mu^+ n_\nu^- \mathcal{M}_{\mu\nu}^{ab} = \frac{x_1 x_2 s}{2 |\vec{q}_{\perp 1}| |\vec{q}_{\perp 2}|} n_\mu^+ n_\nu^- \mathcal{M}_{\mu\nu}^{ab}.$$

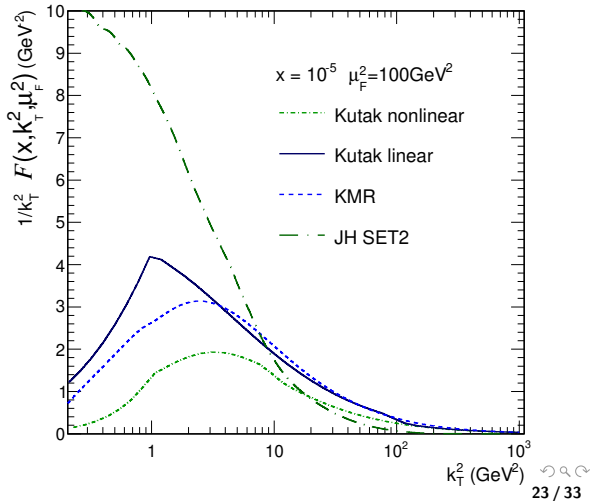
In covariant form, the matrix element reads:

$$\mathcal{M}_{\mu\nu}^{ab} = (-i) 4\pi \alpha_s \epsilon_{\mu\nu\alpha\beta} q_1^\alpha q_2^\beta \frac{\text{Tr}[t^a t^b]}{\sqrt{N_c}} I(\vec{q}_{\perp 1}^2, \vec{q}_{\perp 2}^2).$$

Unintegrated gluon densities

$$xg(x, \mu_f) \propto \int^{\mu_F} dk_{\perp}^2 \frac{\mathcal{F}(x, k_{\perp}^2, \mu_F^2)}{k_{\perp}}$$

Figure:
Unintegrated gluon
densities at scale
 $\mu_F^2 = 100 \text{ GeV}^2$
typical for $\eta_c(1S)$
production in
proton-proton
collisions.



LHCb kinematics $2 < y < 4.5$, $p_T > 6.5 \text{ GeV}$

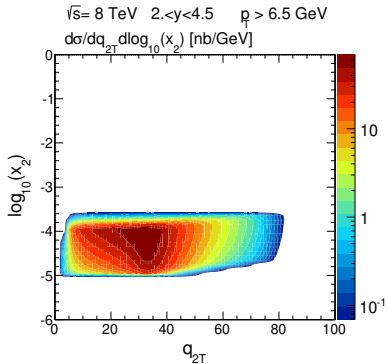
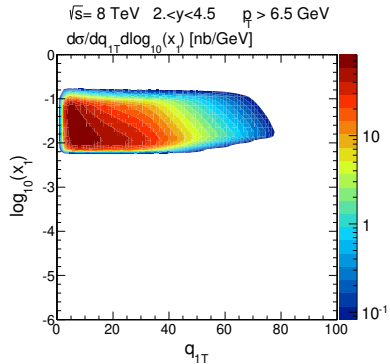


Figure: Distributions in gluon transverse momentum: q_{1T} or q_{2T} and the logarithm of the momentum fraction: $\log_{10}(x_1)$, $\log_{10}(x_2)$

prompt $pp \rightarrow \eta_c(1S)$ - different potential models

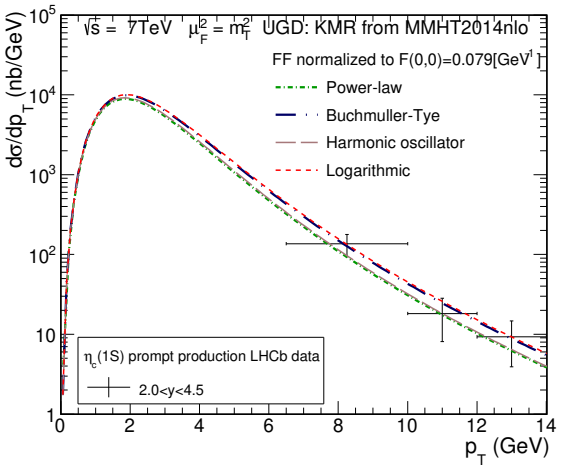


Figure: Differential cross-section in transverse momentum of the meson $\eta_c(1S)$ for different potential models (I. Babiarz, R. Pasechnik, W. Schäfer, A. Szczurek *JHEP02, 037(2020)*)

LHCb Collaboration R. Aaij et al., Eur.Phys.J.C 75 (2015) 7, 311, 1409.3612 [hep-ex]

prompt $pp \rightarrow \eta_c(1S)$

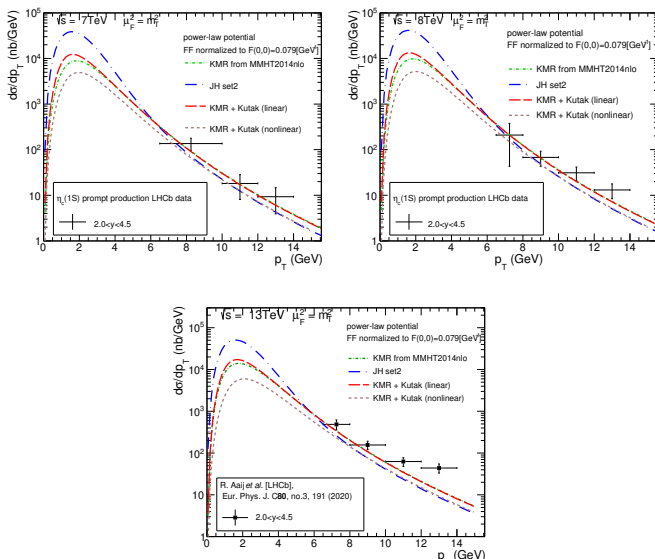


Figure: data: LHCb Collaboration, R. Aaij et al., Eur.Phys.J.C 75 (2015) 7, 311

LHCb Collaboration, R. Aaij et al., Eur.Phys.J.C 80 (2020) 3, 191

prompt $pp \rightarrow \eta_c(2S)$

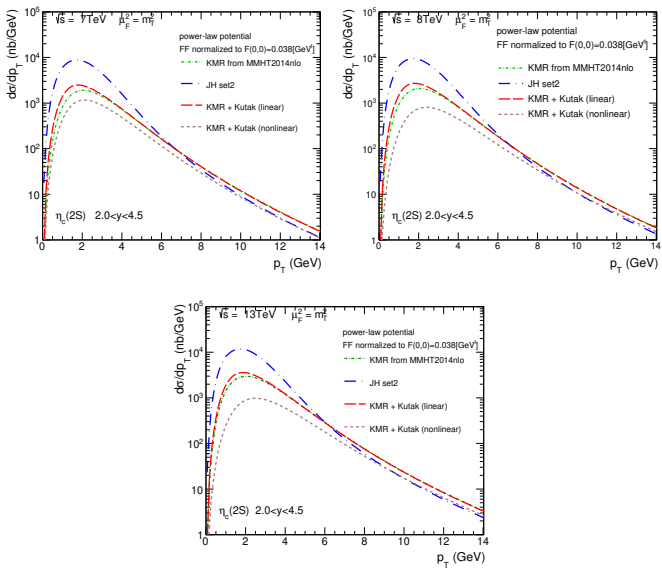
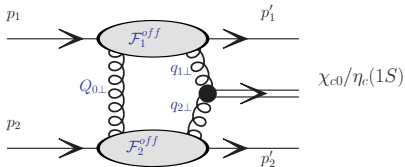


Figure: Differential cross-section as a function of η_c (2S) transverse momentum for $\sqrt{s} = 7, 8 \text{ TeV}$ (top inlays) and 13 TeV (bottom).

Central exclusive production



Generic diagram for **central exclusive production** of η_c and χ_{c0} ,
Phys. Rev. D **102**, 114028 (2020)

$\mathcal{V}^{c_1 c_2} \Rightarrow \mathcal{V}^{c_1 c_2}(g^* g^* \rightarrow \eta_c(1S))$
Prompt hadroproduction of $\eta_c(1S, 2S)$ in the k_T -factorization approach,
JHEP **02**, 037 (2020),

$\mathcal{V}^{c_1 c_2} \Rightarrow \mathcal{V}^{c_1 c_2}(g^* g^* \rightarrow \chi_{c0}(1P))$
Hadroproduction of scalar P-wave quarkonia in the light-front k_T -factorization approach *JHEP* **06**, 101 (2020)

$$\mathcal{M} = \frac{s}{2} \pi^2 \frac{1}{2} \frac{\delta_{c_1 c_2}}{N_c^2 - 1} \int d^2 \mathbf{Q} \mathcal{V}^{c_1 c_2} \frac{\mathcal{F}_g^{\text{off}}(x_1, x', \mathbf{Q}^2, \vec{q}_{\perp 1}^2, \mu^2, t_1) \mathcal{F}_g^{\text{off}}(x_2, x', \mathbf{Q}^2, \vec{q}_{\perp 2}^2, \mu^2, t_2)}{\mathbf{Q}^2 \vec{q}_{\perp 1}^2 \vec{q}_{\perp 2}^2},$$

Durham model of CEP, *Int. J. Mod. Phys. A* **29**, 1430031 (2014), [arXiv:1405.0018 [hep-ph]]

$$\sigma = \frac{1}{2s} \frac{1}{2^8 \pi^4 s} \int |\mathcal{M}|^2 dt_1 dt_2 dy d\phi.$$

$t_1 = (p_1 - p'_1)^2$, $t_2 = (p_2 - p'_2)^2$ and $\phi \in (0, 2\pi)$

R. S. Pasechnik, A. Szczurek, and O. V. Teryaev,
Phys. Rev. D **78**, 014007 (2008),

Off-diagonal gluons

KMR off-diagonal gluon:

Int. J. Mod. Phys. A **29**, 1430031 (2014),

[arXiv:1405.0018 [hep-ph]],

Eur. Phys. J. C **35**, 211–220 (2004)

$$\mathcal{F}_{g,\text{KMR}}^{\text{off}}(x_i, x', Q_{\perp}^2, q_{i\perp}^2, \mu^2, t_i) = R_g \frac{d}{d \ln q_{\perp}^2} \left[x g(x, q_{\perp}^2) \sqrt{T_g(q_{\perp}^2, \mu^2)} \right]_{q_{\perp}^2 = Q_{\perp}^2} F(t),$$

$Q_{i\perp}^2 = \min(Q_{\perp}^2, q_{i\perp}^2)$, $i = 1, 2$ - Durham prescription

$Q_{i\perp}^2 = \sqrt{Q_{\perp}^2 q_{i\perp}^2}$ $i = 1, 2$ - BPSS prescription

CDHI off-diagonal gluon:

Eur. Phys. J. C **61**, 369–390 (2009)

$$\mathcal{F}_{g,\text{CDHI}}^{\text{off}}(x_i, x', Q_{\perp}^2, q_{i\perp}^2, \mu^2, t_i) =$$

$$R_g \left[\frac{\partial}{\partial \log \bar{Q}^2} \sqrt{T_g(\bar{Q}^2, \mu^2)} x g(x, \bar{Q}^2) \right] \cdot \frac{2Q_{\perp}^2 q_{\perp}^2}{Q_{\perp}^4 + q_{\perp}^4} \cdot F(t),$$

$$F(t) = \exp \left(\frac{bt}{2} \right), \quad b = 4 \text{ GeV}^{-2},$$

PST off-diagonal:

Phys. Rev. D **78**, 014007 (2008).

$$\begin{aligned} \mathcal{F}_{g,\text{PST}}^{\text{off}}(x_i, x', Q_{\perp}^2, q_{i\perp}^2, \mu^2, t_i) &= \\ &\sqrt{Q_{\perp}^2 f_g^{\text{GBW}}(x', Q_{\perp}^2) q_{\perp}^2} f_g^{\text{GBW}}(x, q_{\perp}^2) \\ &\times \sqrt{T_g(q_{\perp}^2, \mu^2)} F(t), \end{aligned}$$

$$f_g^{\text{GBW}}(x, q_{\perp}^2) = \frac{3 \sigma_0}{4 \pi^2 \alpha_s} R_0^2 q_{\perp}^2 \exp[-R_0^2 q_{\perp}^2],$$

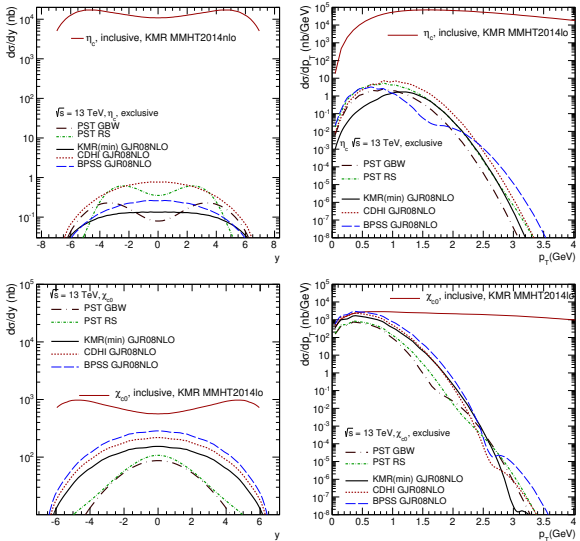
J.HighEnergyPhys.03(2018)102.

$$\begin{aligned} f_g^{\text{RS}}(x, |\vec{q}_{\perp}|) &= \vec{q}_{\perp}^2 \frac{\sigma_0}{\alpha_s} \frac{N_c}{8\pi^2} \\ &\times \int_0^\infty r dr J_0(|\vec{q}_{\perp}|r) \left(1 - \frac{\sigma(x, r)}{\sigma_0} \right). \end{aligned}$$

Phys. Rev. D **88**, 074016 (2013)

$$\begin{aligned} T_g(q_{\perp}^2, \mu^2) &= \exp \left[- \int_{q_{\perp}^2}^{\mu^2} \frac{d\vec{k}_{\perp}^2}{\vec{k}_{\perp}^2} \frac{\alpha_s(k_{\perp}^2)}{2\pi} \right. \\ &\times \left. \int_0^{1-\Delta} \left[z P_{gg}(z) + \sum_q P_{qg}(z) \right] dz \right], \\ \mu^2 &= M^2 + q_{\perp}^2. \end{aligned}$$

Exclusive vs. inclusive distributions



Absorptive correction to $pp \rightarrow pVp$ processes

$$\mathcal{M}(Y, y, \vec{p}_{\perp 1}, \vec{p}_{\perp 2}) = \mathcal{M}^{(0)}(Y, y, \vec{p}_{\perp 1}, \vec{p}_{\perp 2}) - \delta \mathcal{M}(Y, y, \vec{p}_{\perp 1}, \vec{p}_{\perp 2}),$$

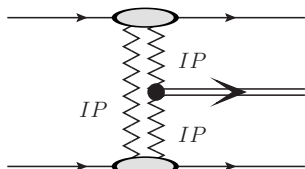
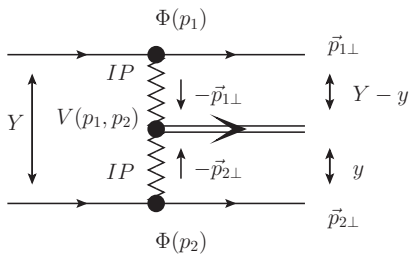
$$\begin{aligned} \mathcal{M}^{(0)}(Y, y, \vec{p}_{\perp 1}, \vec{p}_{\perp 2}) &= i s \Phi_1(\vec{p}_{\perp 1}) R_{\mathbf{P}}(Y-y, \vec{p}_{\perp 1}^2) \\ &\times V(\vec{p}_{\perp 1}, \vec{p}_{\perp 2}) R_{\mathbf{P}}(y, \vec{p}_{\perp 2}^2) \Phi_2(\vec{p}_{\perp 2}) \end{aligned}$$

$$\delta\mathcal{M}(Y, 0, \vec{p}_{+1}, \vec{p}_{+2}) =$$

$$\int \frac{d^2 \vec{k}_\perp}{2(2\pi)^2} T(s, \vec{k}_\perp) \exp \left(-\frac{1}{2} B_D (\vec{p}_{\perp 1} + \vec{k}_\perp)^2 \right)$$

$$T(s, \vec{k}_\perp) = \sigma_{\text{tot}}^{pp}(s) \exp\left(-\frac{1}{2} B_{\text{el}}(s) |\vec{k}_\perp|^2\right)$$

$\sqrt{s} = 13 \text{ TeV} \Rightarrow \sigma_{\text{tot}}^{pp} = (110.6 \pm 3.4) \text{ mb}$,
 $B_{\text{el}} = (20.36 \pm 0.19) \text{ GeV}^{-2}$
G. Antchev *et al.* [TOTEM
Collaboration],
Eur. Phys. J. C **79**, no.2, 103 (2019)



Gap survival probability at mid rapidity

χ_{c0}	$\frac{d\sigma}{dy}_{\text{tot}} _{y=0}$ [nb]	$\frac{d\sigma}{dy}_{\text{tot}}^{\text{abs}} _{y=0}$ [nb]	$S_{y=0}^2$
PST GBW	17	3.7	0.22
PST RS	21	4.5	0.21
CDHI GJR08NLO	42	7.5	0.18
KMR GJR08NLO	29	3.7	0.13
BPSS GJR08NLO	61	8.0	0.13

$$S^2 \equiv \frac{d\sigma/dy|_{y=0}}{d\sigma_{\text{Born}}/dy|_{y=0}}$$

η_c	$\frac{d\sigma}{dy}_{\text{tot}} _{y=0}$ [nb]	$\frac{d\sigma}{dy}_{\text{tot}}^{\text{abs}} _{y=0}$ [nb]	$S_{y=0}^2$
PST GBW	1.8×10^{-2}	3.9×10^{-3}	0.22
PST RS	9.0×10^{-3}	1.9×10^{-3}	0.21
CDHI GJR08NLO	1.8×10^{-1}	4.0×10^{-2}	0.22
KMR GJR08NLO	1.3×10^{-1}	3.0×10^{-2}	0.23
BPSS GJR08NLO	5.8×10^{-2}	2.2×10^{-2}	0.38

Conclusions

- The transition form factor for different wave functions obtained as a solution of the Schrödinger equation for the $c\bar{c}$ system for different phenomenological $c\bar{c}$ potentials from the literature, was calculated.
- We have studied the transition form factors for $\gamma^*\gamma^* \rightarrow \eta_c$ (1S,2S) for two space-like virtual photons, which can be accessed experimentally in future measurements of the cross section for the $e^+e^- \rightarrow e^+e^-\eta_c$ process in the double - tag mode.
- The transition form factor for only one off-shell photon as a function of its virtuality, was studied and compared to the BaBar data for the $\eta_c(1S)$ case.
- Dependence of the transition form factor on the virtuality was studied and the delayed convergence of the form factor to its asymptotic value $\frac{8}{3}f_{\eta_c}$ as predicted by the standard hard scattering formalism, was presented.
- There is practically no dependence on the asymmetry parameter ω , which could be verified experimentally at Belle 2.
- In our calculation of absorptive corrections, we restricted ourselves to the so-called elastic rescattering correction.
- Depending on the gluon distribution used, we obtain for the χ_c the gap survival values of $S^2 = (0.13 - 0.21)$, while for the η_c production, they are somewhat higher, $S^2 = (0.21 - 0.38)$.